OPEN ACCESS Freely available online

Journal of
Microbial & Biochemical Technology

Research Article

Expression and Applications of HriCFP in *E. coli*: A Novel Biosensing Fluorescent Protein

Hira Mehreen[1], Salma Saeed[1], Umut Gerlevik[2], Aamira Tariq[1], Ugur Sezerman[2], Zobia Noreen[1], Xunli Zhang[3], Sammer-ul Hassan[3], Habib Bokhari[1]*

[1]Department of Biosciences, Comsats University Islamabad Campus, Islamabad, Pakistan; [2]Department of Biostatistics and Medical Informatics, Faculty of Medicine, Acibadem University, Istanbul, Turkey; [3]Department of Mechanical Engineering, Faculty of Engineering and Physical Sciences, University of Southampton, United Kingdom

ABSTRACT

Metalloids and heavy metal contamination in the environment have become a global problem. Therefore, there is a dire need to develop effective and inexpensive approaches that can facilitate efficient monitoring of the hazardous level of these environmental pollutants. Microbial cell-based and fluorescent protein-based biosensors offer relatively convenient and inexpensive tools for the analysis of environmental pollutants as opposed to traditional instrumental approaches. Small size fluorescent proteins can withstand exposure to denaturants, high temperature and a wide pH range. These characteristics, along with their potential of sensing different toxic analytes, makes them a suitable candidate for developing on-site detection biosensors. The current study exploits the biosensing potential of a novel fluorescent protein called HriCFP. HriCFP was expressed in the prokaryotic system (gram-negative *E. coli*), which showed stable and discreet expression in bacterial cells. Whole-cell biosensors (WCB) were developed by immobilization of HriCFP expressing non-pathogenic *E. coli via* nitrocellulose membrane, low melting agarose and sodium silicate gel. These immobilized biosensors were tested for their sensitivity of detection for environmental pollutants, i.e., heavy metals (Cu(II), Hg(II), As(III)). These WCBs exhibited profound fluorescent quenching when exposed to a range of heavy metals. These biosensors remained active for 12 days at 4°C, demonstrating their potential for long-term stability and storage. This study implies that HriCFP may have a significant advantage over other larger and multimeric proteins as it has a minimal impact on host strain metabolism and hence, increasing its sustainability for a longer period.

Keywords: Microbiology; Biosensor; Metalloids; Heavy metals; HriCFP; Water pollution; Microbial cell-based; Fluorescent protein-based biosensors; Environmental pollutants

INTRODUCTION

Environmental pollutants such as heavy metals pose a serious threat to human health [1]. Heavy metals are naturally occurring elements; however, majority of the environmental contamination is a result if anthropogenic activities like mining, domestic and industrial use of metals and metal-containing compounds [2,3]. Heavy metals are usually regarded as trace elements primarily because of their presence in trace concentration ranging from 10 µg/L (ppb) to less than 10 mg/L (ppm) [4]. The World Health Organization (WHO) permissible limit of heavy metals and metalloid like copper (Cu), mercury (Hg) and arsenic (As) are 2mg/L, 6 µg/L and 0.01 mg/L respectively in drinking water [5]. Conventional techniques like ion exchange, chelation, chemical precipitation, membrane separation [6] and inductively coupled mass spectrometry, UV visible spectrometry are although precise but too expensive [7]. Therefore, in order to prevent the adverse health and environmental hazards due to heavy metal contamination, careful environmental monitoring of pollutants is required. Living cells such as microbes can detect and process diverse signals, and their self-replication present a lucrative platform to engineer scalable and inexpensive biosensing devices for environmental monitoring [8,9]. Microbial biosensors are either engineered or naturally occurring microorganisms that produce a detectable or visual signal on environmental stimulus [10]. A variety of target analytes like heavy metals, metalloids (As, Cd, Zn, Ni, Cu, Cr, Cu), nutrients, organic xenobiotics have been detected by using whole-cell biosensors [10]. Different metal-specific bacterial sensors were

***Corresponding to**: Habib Bokhari, Department of Biosciences, Comsats University Islamabad Campus, Islamabad, Pakistan, Email: habib@comsats.edu.pk

Received Date: June 15, 2020; **Accepted date:** July 10, 2020; **Published date:** July 17, 2020

Citation: Mehreen H, Saeed S, Gerlevik U Tariq A, Sezerman U, Noreen Z (2020) Expression and Applications of HriCFP in *E. Coli*: A Novel Biosensing Fluorescent Protein. J Microb Biochem Technol. 12:434 doi: 10.35248/1948-5948.20.12.434

previously developed by fusing the reporter gene with different metal regulatory protein-coding genes [11].

Fluorescent protein (FP) based metal sensors have recently emerged as a cheap and simple approach for heavy metal detection [1]. They are unique as no enzymatic modification or cofactors are required for their activation and the formation of functional structures. The GFP-like coral proteins exhibit a broad spectral diversity ranging from blue, green, yellow and red FPs [12], as well as non-fluorescent chromo-proteins [13]. The expression and stability of these wild type FPs can be further optimized by amino acids substitutions possessing favorable optical and biophysical properties. These modifications may ensure a better rate of maturation and reduced sensitivity to pH. The increased stability of the diverse FPs or preferably smaller or monomeric forms has enhanced their demand to be used as optical or fusion tags. Both natural and recombinant fluorescent protein-expressing bacteria have employed as a potential alternative strategy for detection of heavy metals such as Pb(II), Cd(II) and Cu(II) [14,15]. Genetically encoded fluorescent proteins such as GFP, DsRed, YFP and others have been exploited by using different protein engineering and mutagenesis approaches for diverse functional applications. Engineered GFP with the addition of histidine and metal-binding residues around the chromophore region has been documented as an efficient Cu(II) sensor [16]. Similarly, the introduction of Cys in the GFP chromophore enabled the protein to detect heavy metals like Pb(II) and Hg(II) respectively [17,18]. Many new fluorescent proteins like Cu(II) sensing far-red protein (HcRed) from *Hetractis crispa* [19] and recombinant GFP from *Anemonia sulcata* as Cu(II) and Hg (II) sensor [20] are isolated from aquatic marine organisms. Moreover, flavin mononucleotide (FMN) chromophore based protein iLOV was reported as a Cu(II) sensor [21].

We have shown in our previous studies that HriCFP and HriGFP [15,22] can be successfully expressed and purified using an *E. coli* expression system like many other GFP-like proteins. HriCFP (133 amino acids), a monomer FP, is small enough to tag proteins without affecting their folding or function, and cellular processes and interactions in cells can be monitored without interferences. HriCFP may also be superior over larger proteins because of the minimal impact on host strain metabolism enabling additional resources for recombinant target protein production [23]. In the present study, the expression potential of HriCFP in the prokaryotic system (E. coli BL21DE3 cells) was evaluated. The minimum inhibitory concentration (MIC) of these cells for heavy metals like Cu (4.5mM or 7.6g/L) Furthermore, the biosensing capability of this novel fluorescent protein was exploited for the detection of environmental pollutants, *i.e.*, heavy metals (*i.e.*, As, Cu, Hg) was studied.

MATERIAL AND METHODS

All the materials used for this study were of analytical grade. Stock solutions of Copper and Mercury were prepared from their respective chloride salts (Sigma), whereas Arsenite solution was prepared from Sodium arsenite (NaAsO2 Sigma). The glassware used was first cleaned by treatment with nitric acid (15%) for 24 h to remove trace elements, followed by sterilization after autoclaving at 121°C for 20 min.

Expression of HriCFP in *E. coli*

The HriCFP gene was cloned into pET28a+ vector and transformed into *E. coli* (BL21DE3, MoBiTec, Goettingen, Germany) cells. The bacterial cells were induced by using vector Isopropyl β- d-1-thiogalactopyranoside (IPTG) as the vector pET28a+ has a T7 lac promoter. IPTG is a molecular mimic of allolactose which can induce expression of the gene (HriCFP in this case) lying downstream of the lac operon. The HriCFP pet28+ construct was directly transformed in *E. coli* (BL21DE3 cells). The transformed cells were then streaked on agar plates with 30 µL induced culture with 0.3 mM IPTG. Then 0.1% Kanamycin was added as a resistant marker in the medium. The plates were incubated at 37°C overnight, and a portion of these plates was visualized under a fluorescent microscope on a glass slide. Uninduced broth culture was setup by inoculating the HriCFP expressing *E. coli* in 5 mL Luria broth (LB) with 5 µL antibiotic, *i.e.* kanamycin as a selection marker for uninduced culture. Induced broth culture was set up by inoculating 1 mL Hepes buffer (7.0 pH), 5 µL antibiotic (kanamycin) and 5 µL IPTG. The cultures were left in a shaking incubator at 37°C for 16 to 18 hours. After obtaining optical density (OD) 1.00 at 600 nm, the culture was centrifuged in a falcon at 140000 rpm for 5 min followed by discarding the supernatant. The cell pellet was harvested after induction of 5 hours. The pellet was then used for the following immobilization experiments [24].

Immobilization of HriCFP expressing *E. coli* onto a nitrocellulose membrane

The nitrocellulose membrane was cut into 5 mm diameter pieces. The 50 µL bacterial cells (~ $8.0x10^8$ CFU) from an overnight culture were placed onto the nitrocellulose membrane. The membrane was then coated with 4% Na-alginate and was finally submerged in a solution of 0.15% Calcium chloride ($CaCl_2$) for final cross-linking. This treatment made a layer of Ca-alginate on the membrane. The treated nitrocellulose membranes were visualized under a UV hand lamp of range 315- 400 nm, as described previously [25].

Immobilization of HriCFP expressing *E. coli* using low melting agarose

The HriCFP expressing *E. coli* (BL21DE3 cells) with a 0.02 OD at 600 nm and $1.6x10^7$ CFU was immobilized in low melting agarose by modifying the mammalian cancer cells anchorage-independent soft agar colony formation assay as described previously [26,27]. The colonies were visualized after 24 hours under UV (315- 400 nm).

Immobilization of HriCFP expressing *E. coli* using sodium silicate

Sodium silicate 1g was mixed with 6 mL of de-ionized distilled water. The mixture was then incubated at 70°C until a colloidal solution was formed (10-12 min). The solution was then poured in a petri dish and allowed to cool at room temperature. The 6 mL of bacterial culture (0.8 OD at 600 nm) was mixed with a sodium silicate solution in a petri dish. The pH was adjusted to 8.0 by using 0.75 M citric acid; approximately 1.8 mL of citric acid was used to form a gel. The gel formation was achieved in 2 min [28].

Heavy metals biosensing capability test

The biosensing capability of these bacterial cultures was tested by exposing the overnight culture with OD 0.8-1 nm to different concentrations (100-300 µg/L) of heavy metals such as Cu(II), Hg(II) and As(III). These cultures were also tested against different concentrations of monovalent cations like Sodium and potassium (100-300 µg/L). De-ionized water and bacterial cells unexposed

to heavy metals were used as a control. Direct visualization of the quenching effect was done using a handheld UV lamp.

Homology modelling and quality check

Homology based three-dimensional models of HriCFP (134 amino acids) with full coverage were created by using various tools, *i.e.* i-TASSER [29], MODELLER 9.21 [30], Phyre2 [31], RaptorX [32] and Robetta [33] with different templates. Then, all these models were compared in terms of structural quality based on the known high-quality structures by using the algorithms in SAVES v5.0 web server (https://servicesn.mbi.ucla.edu/SAVES/) such as Verify3D [34,35], ERRAT [36], Prove [37], PROCHECK [38], WHATCHECK [39], and similarity to existing fluorescent protein structures in RCSB PDB database (http://www.rcsb.org/pdb/) [40]. Visualizations were performed by UCSF Chimera [41].

Metal-binding site predictions

IonCom [42], MetalDetector v2.0 [43], MIB [44] and Metsite [45] algorithms were used on their webservers to predict the possible metal ion binding sites in the protein structure. Of note, none of these predictors has a prediction algorithm for arsenic, whereas all have for copper. MIB also has an algorithm for mercury binding site prediction. MetalDetector has a general focus on transition metals. IonCom also predicts sodium and potassium ion binding sites.

RESULTS AND DISCUSSIONS

Expression of HriCFP in *E. coli* and *Bacillus megaterium*

HriCFP was successfully transformed and expressed in *E. coli* (BL21DE3 cells). The cells showed an increase in fluorescence after IPTG induction. Figure 1 shows the difference in fluorescence between the uninduced and induced cells. The induced cells showed a stable and bright cyan fluorescence when exposed under UV (350 nm).

Heavy metal detection using HriCFP

The stable fluorescence offered by these bacteria further urged us to investigate their behavior towards metal ions. HriCFP producing bacteria were directly exposed to heavy metals, and fluorescence quenching was observed on exposure to heavy metals like As(III), Cu(II) and Hg(II) at 300µg/L concentration. No, fluorescence quenching was observed in the case of monovalent cations such as Na(I) and K(I).

We further immobilized these fluorescent protein-producing bacterial cells, using nitrocellulose and low melting agarose. The immobilized bacteria bearing nitrocellulose chips on exposure to heavy metals like copper, mercury and arsenic exhibited fluorescence quenching. These chips were able to sense from 100-300 µg/L of these divalent cations. The expression of the fluorescent protein was induced by IPTG. HEPES buffer was added to the media solely for pH stability. The cells showed stable expression until 12 days on nitrocellulose under UV (Figure 2). The calcium alginate layer ensured sustainable and stable CFP expression. Moreover, no quenching was observed in the case of monovalent cations (Table 1). This absence of quenching in case of sodium and potassium might be due to the lack of their binding sites.

Low melting agarose was used for immobilization of HriCFP expressing bacterial cells by modifying the anchorage-independent growth assay for mammalian cancer cells [26,27]. The equal-sized chip of agarose bearing the immobilized HriCFP expressing bacterial cells was dipped in heavy metal Hg(II), Cu(II) and As(III) solutions of different concentration (0.002-2.0mg/L). De-ionized water was used as a control. Strong fluorescence quenching with the increase in the concentration of the divalent cations like Hg(II), Cu(II) was observed (Figure 3). However, a relatively smaller decrease in fluorescence was observed with the corresponding increase in the concentration of the trivalent cation As(III) (Figure 3). The de-ionized water was used as a control, and no fluorescence quenching was observed validating the stability of HriCFP in agarose immobilized bacterial cells (Figure 3). As compared to nitrocellulose, we observed that fluorescence quenching starts at the lapse of 5 minutes; however, it reaches the maximum level after 25 minutes. We presume this might be due to reduced penetration of these ions into the agarose matrix.

The third method was based on immobilizing the whole cells in sodium silicate gel. Here, two of the gel pieces were created, one with the BL21DE3 cells containing a plasmid with HriCFP gene. The second gel piece was made with BL21DE3 cells with plasmid but without HriCFP the gene. This allowed the visualization of glowing and quenching rapidly. In this method, we took 1x1 cm pieces of both the gels with the help of a spatula and placed it on a glass slide, then took 100 µL of 300 µg/L volume from a stock of heavy metal solutions and dropped it on the glowing gel (Fig. 4). After 5 min incubation, the results were visualized under UV (350 nm).

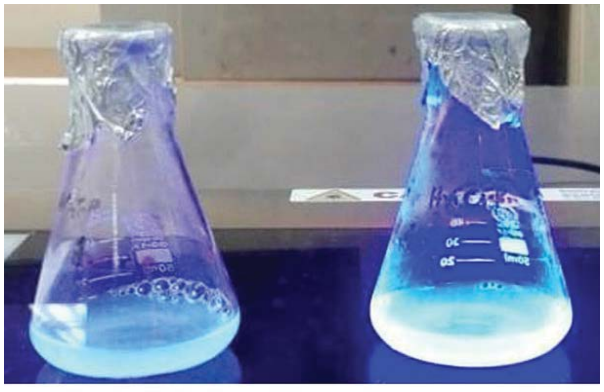

Uninduced **Induced**

Figure 1: Expression of HriCFP: The uninduced culture of BL21DE3 cells expressing HriCFP protein without IPTG showed less fluorescence as compared to the IPTG induced HriCFP expressing cells when visualized under UV (350 nm).

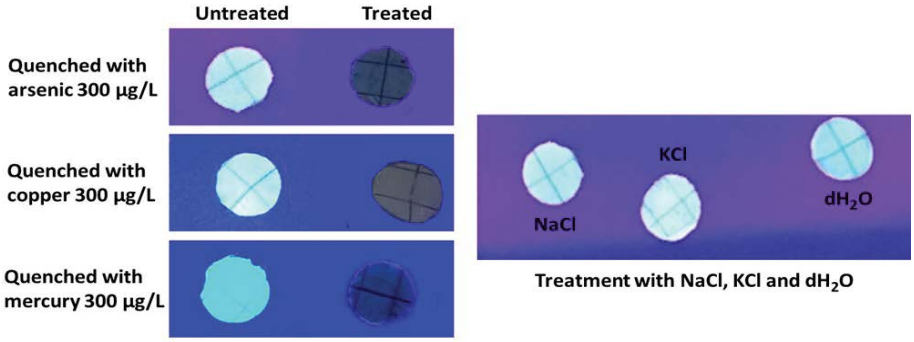

Figure 2: Immobilization of bacterial cells on the nitrocellulose membrane. Cyan fluorescence was observed on IPTG induction under UV. Bio-sensing ability of bacterial cells on the nitrocellulose chips upon exposure to different heavy metals like As(III), Cu(II) and Hg(II) at 300µg/L concentration. No, fluoresce quenching was observed in the case of monovalent cations like Na(I) and K(I).

Table 1: Shows that 100µg/L < amount of heavy metals vanish the glow of cells whereas, with monovalent metals, the glowing effect is still present.

Metals salts	100 µg/L	200 µg/L	300 µg/L
Sodium arsenite	Quenched	Quenched	Quenched
Copper sulphate	Quenched	Quenched	Quenched
Mercuric chloride	Quenched	Quenched	Quenched
Potassium chloride	Glowed	Glowed	Glowed
Sodium chloride	Glowed	Glowed	Glowed

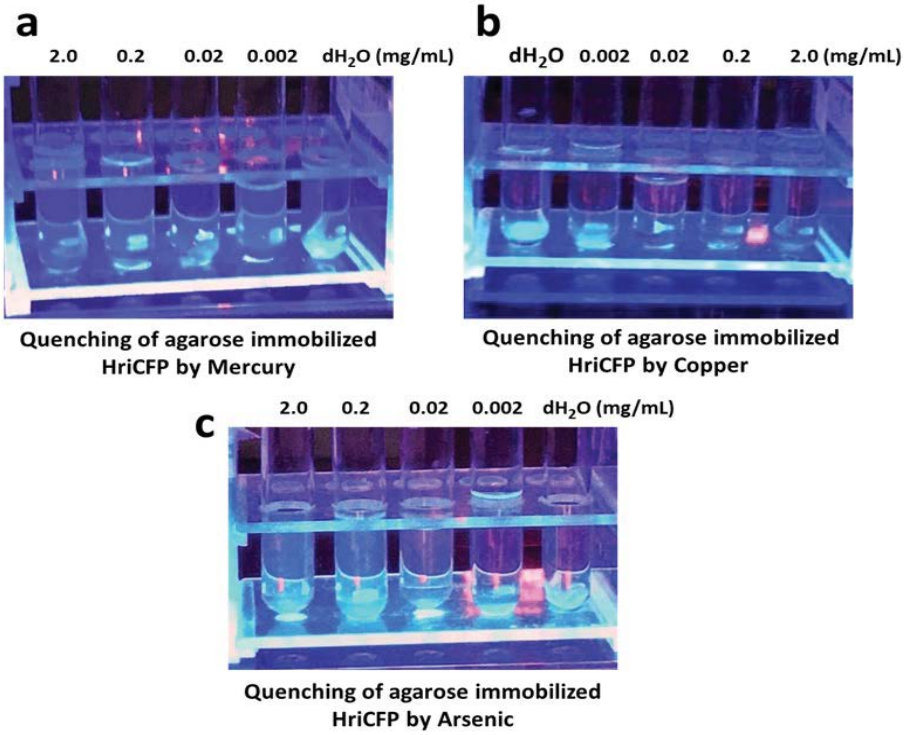

Figure 3: Low melting agarose-based Immobilization of HriCFP producing bacterial cells: The induced HriCFP bacterial cells after immobilization using modified anchorage-independent growth assay were treated with different concentrations of heavy metals. (a). Fluorescence quenching was observed in all tested concentration of Cu(II). The strongest decline in fluorescence was observed at 0.2 and 2.0mg/L concentration of Cu(II)ions. (b) Fluorescence quenching was observed in 0.002, 0.02 and 0.2mg/L concentration of Hg(II) ions. Smaller fluorescence quenching was observed at 2.0mg/L and 2.0 mg/L concentration of Hg(II)ions. (c) A decrease in fluorescence was observed at 0.002 and 0.02mg/L concentration of As(III) ions. However, a slighter decline in fluorescence was observed at higher concentration of 0.2 and 2.0mg/L As(III) ions..

Structural basis of fluorescence quenching mechanism

Supplementary Table 1 illustrates that Robetta model had the best quality scores, and it can be said that the second-best model was MODELLER model, mainly based on the number of "Pass" and the Ramachandran plot analysis. Although Robetta provided the best quality model, the model did not have the standard fluorescent protein structure, which has a chromophore region in the middle of the β-barrel structure. Therefore, the second-best model predicted by the MODELLER was selected due to optimal folding, as shown in Supplementary Figure 1 [46]. This model was built by MODELLER based on the template enhanced cyan fluorescent protein (PDB ID:2wsn) was chosen for further investigations.

Metal-binding sites in HriCFP structure were predicted by several different algorithms, and the predicted metal-binding residues are

shown in Table 2. Metsite uses a combination of structure and sequence information. In contrast, IonCom uses the knowledge on known ion-binding protein structures, and MetalDetector makes a prediction based on Fe/S clusters upon sequence information. At the same time, MIB predicts based on the submitted protein structure by comparing with the metal-binding templates Akcapinar [42-45,47]. As can be seen in Table 2, MIB predicted three different regions for mercury ion and four regions for copper ion while MetalDetector gave four potential residues. IonCom gave no binding sites for copper, sodium and potassium ions. Metsite resulted in a single residue, Asn74, which was profoundly different than the predictions of others. When all these results are considered, MetalDetector and MIB have common three predictions for copper and mercury binding residues (i.e. His17, His60 and His64) although their algorithms are very distinct as mentioned. Therefore, these predicted residues were considered as more reliable than the others. Another supportive information for the binding of these residues is that histidine residues are known with the metal-binding ability [48]. All predicted residues and regions were shown on the model with the chromophore in Figure 5. We propose that the binding of His64 to metals might lead to quenching of the chromophore motif KYG.

As shown in Figure 5, there are many candidate regions for metal-binding in the HriCFP structure, and most of these regions are close to either the chromophore-creating residues or the core of the protein. For these cases, especially for the mentioned high-reliability regions (purple-coloured in Figure 5), it can be expected that the protein structure will be critically affected upon the binding of these divalent transition metal ions in terms of protein folding and chromophore stability. In addition, arsenite is trivalent, whereas sodium and potassium are monovalent.

In the literature, there are many examples of the quenching mechanisms of fluorescent proteins. Moreover, these mechanisms are related to denaturation or disruption of chromophore removal from the β-barrel complex formation with divalent and trivalent metal ions in the solution [1,49,50]. Furthermore, β-barrel disruption mechanism is likely in HriCFP upon the binding of copper, arsenite and mercury since most of the predicted binding sites were found inside the β-barrel, which can critically change the folding of this small fluorescence protein as removing the chromophore from the middle of the β-barrel structure.

CONCLUSIONS

Thus, the HriCFP isolated from *Hydnophora rigida* can be successfully expressed in *E. coli* BL21DE3 cells. The HriCFP expressing bacterial cells were immobilized *via* three different approaches (nitrocellulose, low melting agarose and sodium silicate). The immobilized forms were further tested for heavy metal ions (Cu(II), Hg(II), As(III)) detection. Sodium silicate and nitrocellulose based immobilized bacterial cells showed a steady decrease in fluorescence when treated with different heavy metal ions (Cu (II), Hg (II), As(III)) at 300µg/L concentration. However, with low melting agarose, strong fluorescence quenching was observed in the case of divalent cations (Cu(II), Hg(II) as opposed to trivalent cation As(III). Additionally, the assay required longer incubation time probably due to slow penetration within the agarose matrix. The strongest stability of HriCFP expression was observed in the case of sodium silicate. These immobilized biosensors remained active for 12 days at 4^{0}C, demonstrating its potential for long-term stability. The three-dimensional predicted model of HriCFP also demonstrated metal-binding sites validating the fluorescence

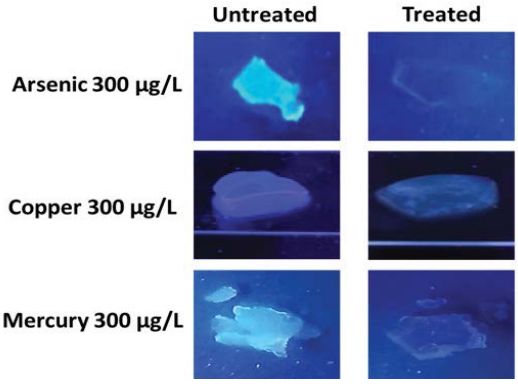

Figure 4: The sodium silicate gel-based immobilized HriCFP expressing bacterial cells showed fluorescence quenching when treated with As(III), Cu(II) and Hg(II) ions at a concentration of 300 µg/L. The untreated panel showed the cyan fluorescence of the HriCFP expressing bacterial cells when left untreated, showing the stability of expression in the immobilized form.

Table 2: Shows the residues in metal-binding sites predicted by the listed algorithms. Only the predictions for metals used in this study were listed below. If the predicted residues are numbered, it indicates that the residues create a binding region together.

Predictor	Metal	Predicted residues
MetalDetector	Cu^{2+}, Hg^{2+}	His17, His44, His60, His64
IonCom	Na^{+}, K^{+}, Cu^{2+}	No binding site detected
Metsite	Cu^{2+}	Asn74
MIB	Hg^{2+}	(1) His60, Phe87, His93, His130 (2) Pro20, Ser21 (3) Phe87, His93
MIB	Cu^{2+}	(1) His17, His60 (2) Gly63, His64, Pro112, His130 (3) His60, Phe87, His93, His130 (4) His93, Ala95, His130

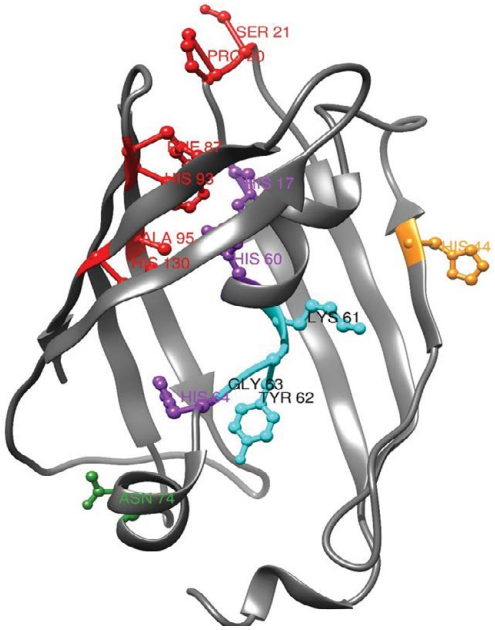

Figure 5: All predicted metal-binding residues and chromophore residues in HriCFP structure. The overall structure was represented as rounded ribbon, whereas the predicted residues were balls and sticks. Chromophore residues with cyan colour, Metsite prediction as forest green, only MetalDetector residues as orange, only MIB predictions with red colour, and the residues predicted by both MetalDetector and MIB were represented with purple colour.

quenching observed on heavy metal ions exposure. Future studies may provide protein engineering-based approaches to circumvent the reduced sensitivity of HriCFP towards arsenite. Furthermore, future quantitative analysis of these techniques combined with fluorescent imaging would lead towards the development of portable biosensors for heavy metal detection from environmental samples.

ACKNOWLEDGEMENT

PI-HB would like to thank Higher Education Commission for providing Funding to carry out this research under the grant number NRPU-3470 titled as " Strengthening Biotechnology Industry in the Country: Developing an Educational Tool Kit for Training Undergraduate Students as well as for Research Purpose: Lab to Commercialization" HM & SS like to thank for financial support for being Research Associates in this project.

CONFLICTS OF INTEREST

Author declared that there is no conflict of study.

REFERENCES

1. Ravikumar Y, Nadarajan SP, Lee C, Jung S, Bae D, Yun H. FMN-based fluorescent proteins as heavy metal sensors against mercury ions. J Microbiol Biotechnol. 2016;26:530-539.
2. Shallari S, Schwartz C, Hasko A, Morel JL. Heavy metals in soils and plants of serpentine and industrial sites of Albania. Sci Total Environ. 1998;209:133-142.
3. He Z, Yang XE, Stoffella PJ. Trace elements in agroecosystems and impacts on the environment. J Trace Elem Med Biol, 2005;19:125-140.
4. Tchounwou PB, Yedjou CG, Patlolla AK, Sutton DJ. Heavy metal toxicity and the environment, in Molecular, clinical and environmental toxicology. Springer. 2012;100:133-164.
5. World Health Organization (WHO). Guidelines for drinking-water quality. WHO chronicle. 2011;38:104-108.
6. Malakootian M, Nouri J, Hossaini H. Removal of heavy metals from paint industry's wastewater using Leca as an available adsorbent. Int J Env Sci Tech. 2009;6:183-190.
7. D'Souza SF. Microbial biosensors. Biosens Bioelectron. 2001;16:337-353.
8. Andreazza R, Pieniz S, Wolf L, Lee M, Camargo FAO, Okeke BC. Characterization of copper bioreduction and biosorption by a highly copper resistant bacterium isolated from copper-contaminated vineyard soil. Sci Total Environ. 2010;408:1501-1507.
9. Chang HJ, Voyvodic PL, Zúñiga A, Bonnet J. Microbially derived biosensors for diagnosis, monitoring and epidemiology. Microb Biotechnol. 2017;10:1031-1035.
10. van der Meer JR, Belkin S. Where microbiology meets microengineering: Design and applications of reporter bacteria. Nat Rev Microbiol. 2010;8:511-522.
11. Ivask A, Hakkila K, Virta M. Detection of organomercurials with sensor bacteria. Anal Chem. 2001;73:5168-5171.
12. Matz MV, Fradkov AF, Labas YA, Savitsky AP, Zaraisky AG, Markelov ML, et al. Fluorescent proteins from nonbioluminescent Anthozoa species. Nat Biotechnol. 1999;17:969-973.
13. Labas YA, Gurskaya NG, Yanushevich YG, Fradkov AF, Lukyanov KA, Lukyanov SA, et al. Diversity and evolution of the green fluorescent protein family. Proc Natl Acad Sci U S A. 2002;99:4256-4261.
14. Arias-Barreiro CR, Okazaki K, Koutsaftis A, Inayat-Hussain SH, Tani A, Katsuhara M, et al. A bacterial biosensor for oxidative stress using the constitutively expressed redox-sensitive protein roGFP2. Sensors (Basel). 2010;10:6290-6306.
15. Bokhari H, Smith C, Veerendra K, Sivaraman J, Sikaroodi M, Gillevet P. Novel fluorescent protein from Hydnophora rigida possess cyano emission. Biochem Biophys Res Commun. 2010;396:631-636.
16. Bálint E, Petres J, Szabó M, Orbán C, Szilágyi L, Ábrahám B. Fluorescence of a histidine-modified enhanced green fluorescent protein (EGFP) effectively quenched by copper (II) ions. J Fluoresc. 2013;23:273-281.
17. Chapleau RR, Blomberg R, Ford PC, Sagermann M. Design of a highly specific and noninvasive biosensor suitable for real-time in vivo imaging of mercury (II) uptake. Protein Sci. 2008;17:614-622.
18. Nadarajan SP, Ravikumar Y, Deepankumar K, Lee C, Yun H. Engineering lead-sensing GFP through rational designing. Chem Commun (Camb). 2014;50:15979-15982.

19. Rahimi, Y, Copper sensing based on the far-red fluorescent protein, HcRed, from Heteractis crispa. Anal Biochem. 2007;370:60-67.

20. Masullo T, Shrestha S, Banerjee T, Deo KS. Development of a biosensor for copper detection in aqueous solutions using an anemonia sulcata recombinant GFP. Appl Biochem Biotechnol. 2014;172:2175-2187.

21. Ravikumar Y, Nadarajan SP, Lee C, Rhee J, Yun H. A new generation fluorescent based metal sensor-iLOV protein. J Microbiol Biotechnol, 2015;25:503-510.

22. Bokhari H, Smith C, Veerendra K, Sivaraman J, Sikaroodi M, Gillevet P. Novel fluorescent protein from Hydnophora rigida possesses green emission. Biochem Biophys Res Commun. 2014;448:33-38.

23. Sambrook J, Russell DW. Calcium-phosphate-mediated transfection of eukaryotic cells with plasmid DNAs. CSH Protoc. 2006;2006:pdb. prot3871.

24. Saeed S, Mehreen H, Gerlevik U, Tariq A, Manzoor A, Noreen Z, et al., HriGFP novel flourescent protein: Expression and applications. Molecular Biotechnology, 2020;65:280-288.

25. Futra D, Heng LY, Ahmed A, Surif S, Ling TL. An optical biosensor from green fluorescent Escherichia coli for the evaluation of single and combined heavy metal toxicities. Sensors (Basel). 2015;15:12668-12681.

26. Jadaliha M, Gholamalamdari O, Tang W, Zhang Y, Petracovici A, Hao Q, et al. A natural antisense lncRNA controls breast cancer progression by promoting tumor suppressor gene mRNA stability. PLoS Genet. 2018;14:e1007802.

27. Tariq A, Hao Q, Sun Q, Singh DK, Jadaliha M, Zhang Y, et al. LncRNA-mediated regulation of SOX9 expression in basal subtype breast cancer cells. RNA. 2020;26:175-185.

28. Alvarez GS, Foglia ML, Copello GJ, Desimone MF, Diaz LE. Effect of various parameters on viability and growth of bacteria immobilized in sol–gel-derived silica matrices. Appl Microbiol Biotechnol. 2009;82:639-646.

29. Zhang Y. I-TASSER server for protein 3D structure prediction. BMC bioinformatics. 2008;9:40.

30. Webb B, Sali A. Comparative protein structure modeling using MODELLER. Curr Protoc Bioinformatics. 2016;54:5.6.1-5.6.37.

31. Kelley LA, Mezulis S, Yates CM, Wass MN, Sternberg MJ. The Phyre2 web portal for protein modeling, prediction and analysis. Nat Protoc. 2015;10:845-858.

32. Peng J, Xu J. RaptorX: exploiting structure information for protein alignment by statistical inference. Proteins. 2011;79:161-171.

33. Kim DE, Chivian D, Baker D. Protein structure prediction and analysis using the Robetta server. Nucleic Acids Res. 2004;32:W526-W531.

34. Lüthy R, Bowie JU, Eisenberg D. Assessment of protein models with three-dimensional profiles. Nature. 1992;356:83-85.

35. Eisenberg D, Lüthy R, Bowie JU. VERIFY3D: Assessment of protein models with three-dimensional profiles. Methods Enzymol. 1997;277:396-404.

36. Colovos C, Yeates TO. Verification of protein structures: Patterns of nonbonded atomic interactions. Protein Sci. 1993;2:1511-1519.

37. Pontius J, Richelle J, Wodak SJ. Deviations from standard atomic volumes as a quality measure for protein crystal structures. J Mol Biol. 1996;264:121-136.

38. Laskowski RA, MacArthur MW, Moss DS, Thornton JM. PROCHECK: A program to check the stereochemical quality of protein structures. J Appl Crystallogr. 1993;26:283-291.

39. Hooft RW, Vriend G, Sander C, Abola EE. Errors in protein structures. Nature. 1996;381:272-272.

40. Berman HM, Westbrook J, Feng Z, Gilliland G, Bhat TN, Weissig H, et al. The protein data bank. Nucleic Acids Res. 2000;28:235-242.

41. Pettersen EF, Goddard TD, Huang CC, Couch GS, Greenblatt DM, Meng EC, et al. UCSF Chimera—A visualization system for exploratory research and analysis. J Comput Chem. 2004;25:1605-1612.

42. Hu X, Dong Q, Yang J, Zhang Y. Recognizing metal and acid radical ion-binding sites by integrating ab initio modeling with template-based transferals. Bioinformatics. 2016;32:3260-3269.

43. Passerini A, Lippi M, Frasconi P. MetalDetector v2. 0: Predicting the geometry of metal binding sites from protein sequence. Nucleic Acids Res. 2011;39:W288-W292.

44. Lin Y, Cheng C, Shih C, Hwang J, Yu C, Lu C. MIB: Metal ion-binding site prediction and docking server. J Chem Inf Model. 2016;56:2287-2291.

45. Sodhi JS, Bryson K, McGuffin LJ, Ward JJ, Wernisch L, Jones DT. Predicting metal-binding site residues in low-resolution structural models. J Mol Biol. 2004;342:307-320.

46. Stepanenko OV, Stepanenko OV, Kuznetsova IK, Verkhusha VV, Turoverov KK. Beta-barrel scaffold of fluorescent proteins: Folding, stability and role in chromophore formation. Int Rev Cell Mol Biol. 2013;302:221-278.

47. Akcapinar GB, Sezerman OU. Computational approaches for de novo design and redesign of metal-binding sites on proteins. Biosci Rep. 2017;37:BSR20160179.

48. Chakrabarti P. Geometry of interaction of metal ions with histidine residues in protein structures. Protein Eng. 1990;4:57-63.

49. Baldridge A, Solntsev KM, Song C, Tanioka T, Kowalik J, Hardcastle K, et al. Inhibition of twisting of a green fluorescent protein-like chromophore by metal complexation. Chem Commun (Camb). 2010;46:5686-5688.

50. Rahimi Y, Goulding A, Shrestha S, Mirpuri S, Deo SK. Mechanism of copper induced fluorescence quenching of red fluorescent protein, DsRed. Biochem Biophys Res Commun. 2008;370:57-61.